

# Structural and Electronic Properties of Buckled Silicon Kagome (SiKL)



Chenhaoyue Wang, Amartya Banerjee

Materials Science & Engineering, University of California, Los Angeles

## Introduction

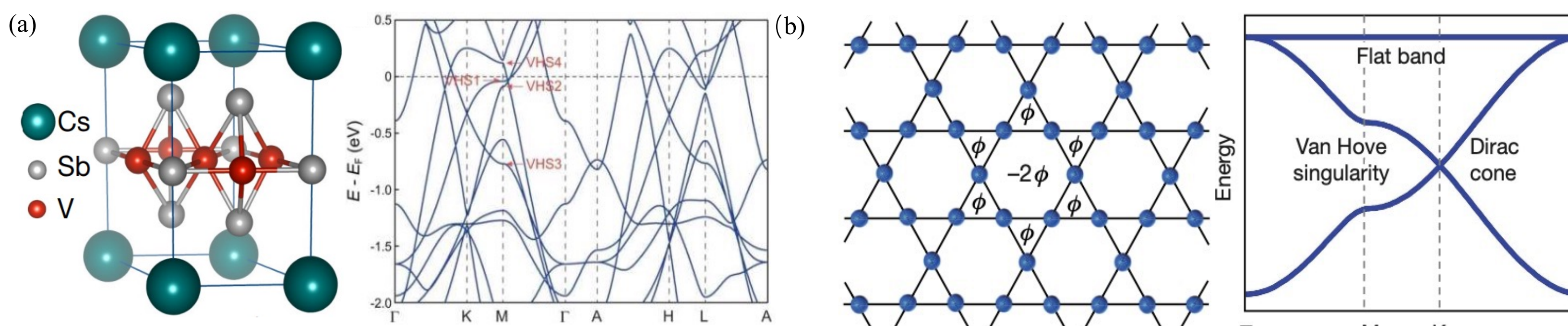


Figure 1. Geometry configurations and corresponding band structure of : (a) a 3D Kagome composite [1] [2]; (b) a 2D single element Kagome lattice [3].

## Carbon Kagome Nanotubes

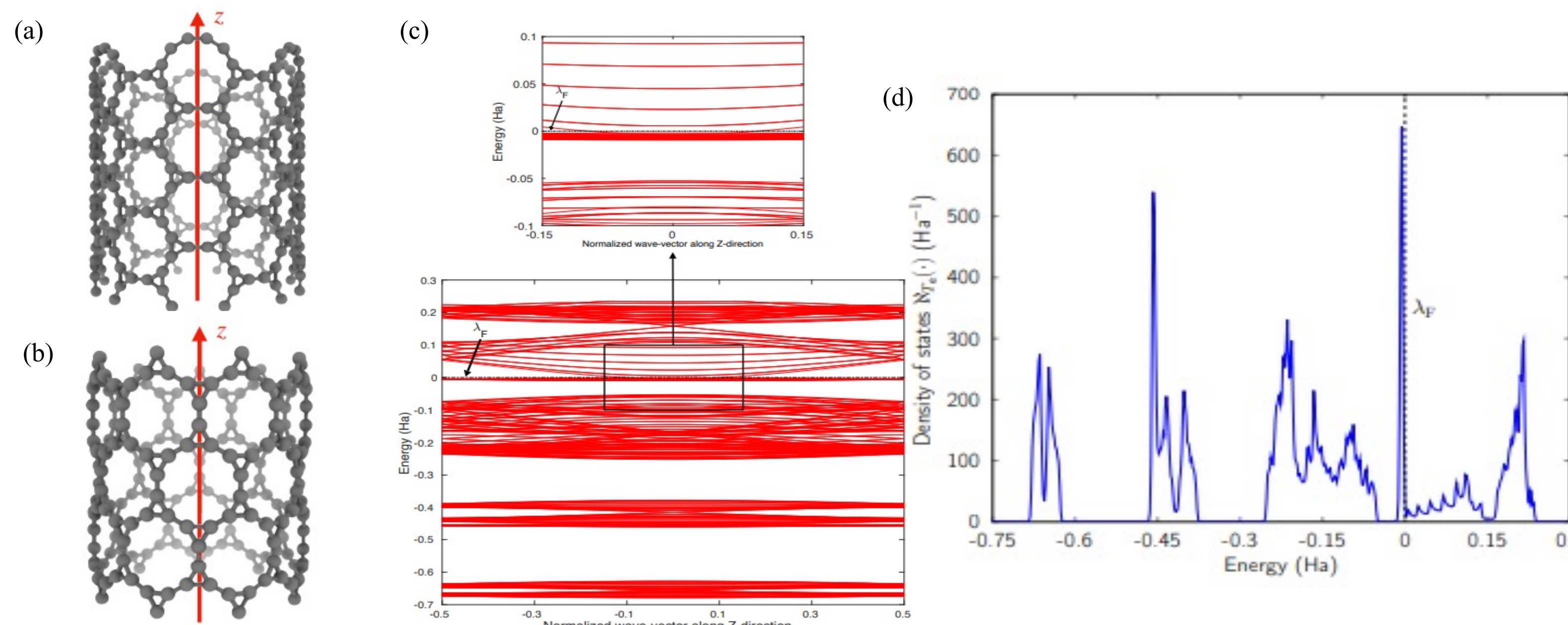


Figure 2. (a) Armchair and (b) zigzag configurations of carbon Kagome nanotubes; (c) corresponding band structure; and (d) density of states (DOS) [4].

## Honeycomb Kagome Structures

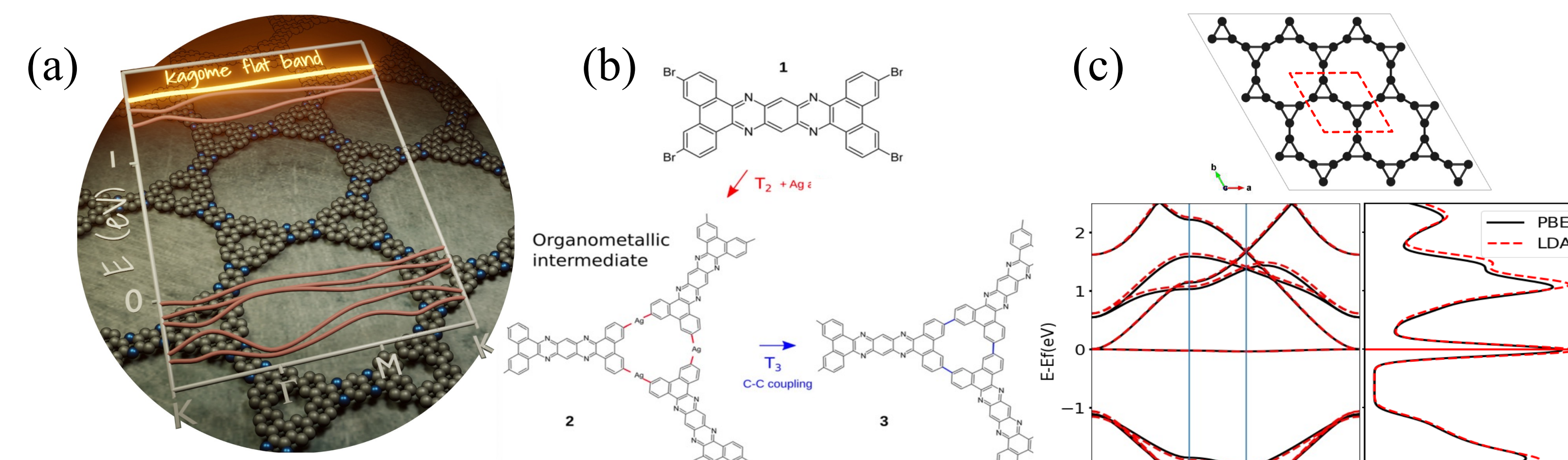


Figure 3. (a) Structure configuration and (b) synthetic route of Kagome graphene[5]; (c) top view of a honeycomb-like Kagome silicon lattice (SiKL) along with its band structure and DOS diagram.

## Structure Searching of Buckled SiKL

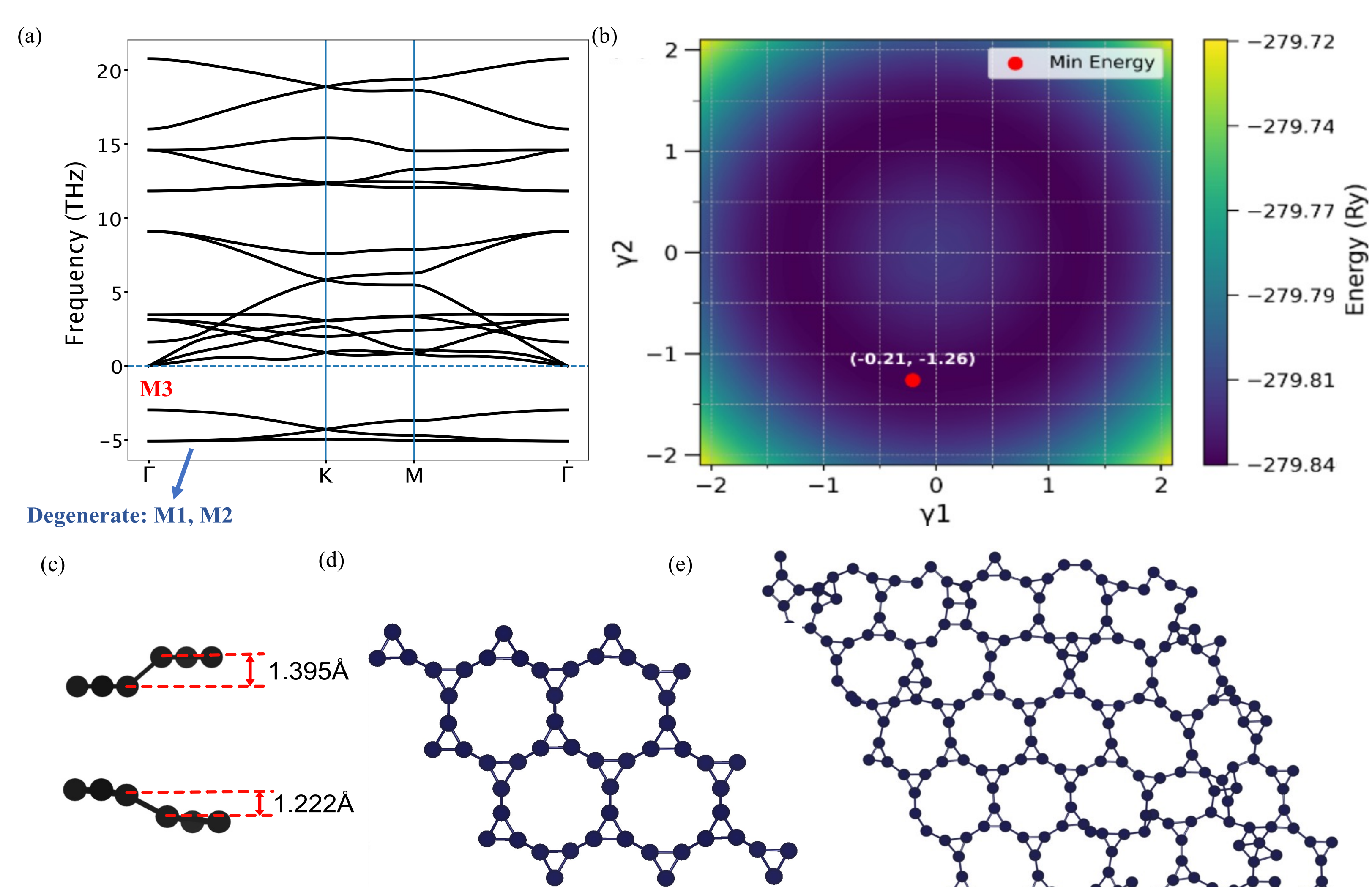


Figure 4. (a) Phonon dispersion of planar SiKL. (b) Energy landscape of the perturbed SiKL structure. (c) Side views of two local energy-minimum configurations of SiKL . Averaged atomic geometries from AIMD calculations at 315K for (d) a  $3 \times 3 \times 1$  superlattice and (e) a  $6 \times 6 \times 1$  superlattice.

## References

- [1] H. Zhao et al., Nature 599, 216 (2021).
- [2] Sargent et al., NCCR MARVEL, (2022).
- [3] J.-X. Yin et al., Hasan, Nature 612, 647 (2022).
- [4] H. M. Yu et al., RSC Advances, 14(2), 963-981 (2024).
- [5] Pawlak, Romy, et al. Angewandte Chemie International Edition, (2021).

## Mechanical Stability of Buckled SiKL

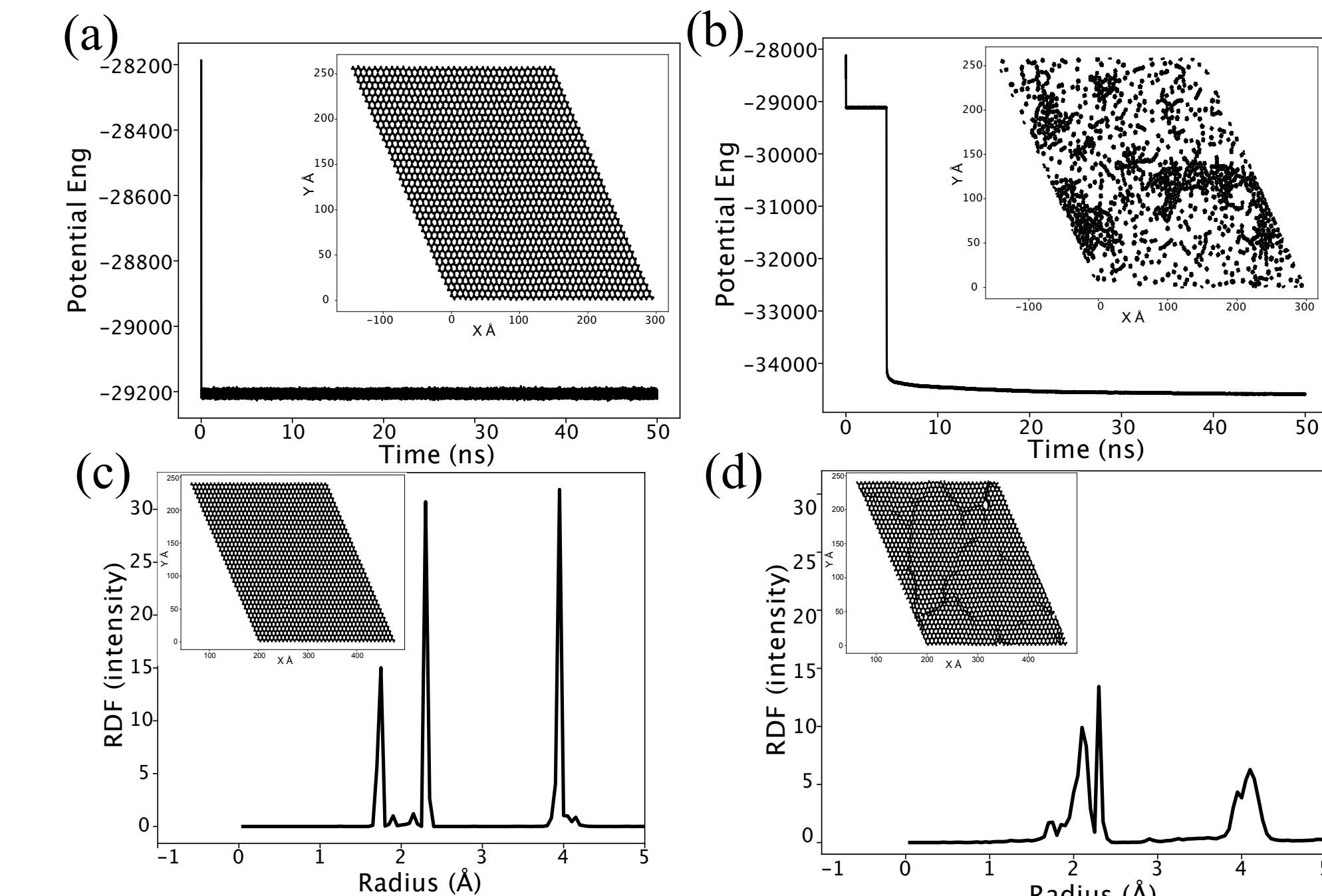


Figure 5. Molecular dynamics (MD) potential energy of buckled SiKL at temperatures (a) below and (b) above the critical temperature  $T_c$ . Radial distribution function (RDF) intensity plots for (c) crystalline and (d) amorphous SiKL.

## Phase Diagram of Buckled SiKL

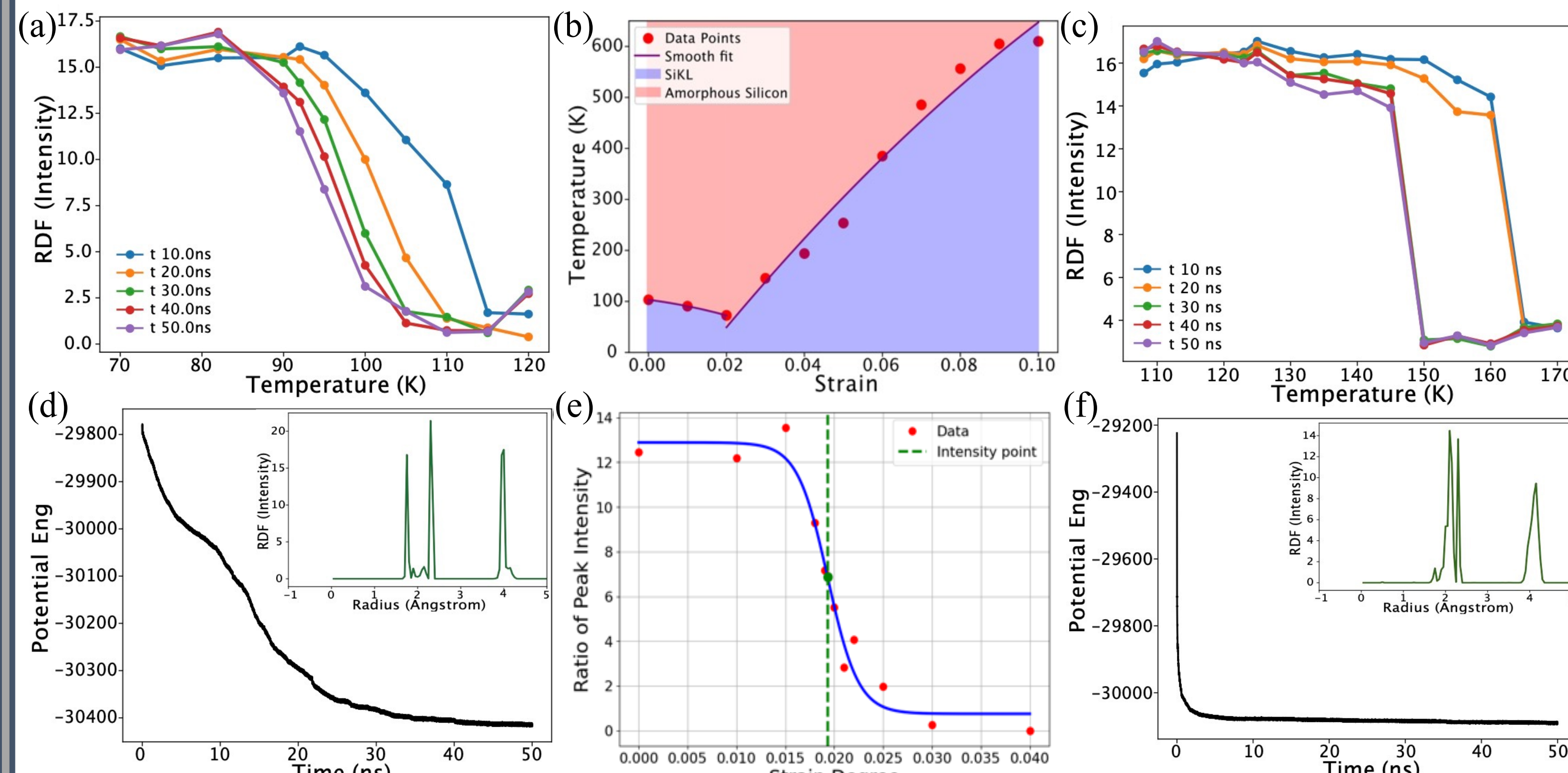


Figure 6. RDF intensity as a function of temperature for buckled SiKL at (a, d) low strain and (c, f) high strain. (b) Phase diagram of SiKL as a function of strain and temperature. (e) Ratio of primary to secondary crystalline peaks as a function of strain.

## Buckled SiKL Growth on Silver

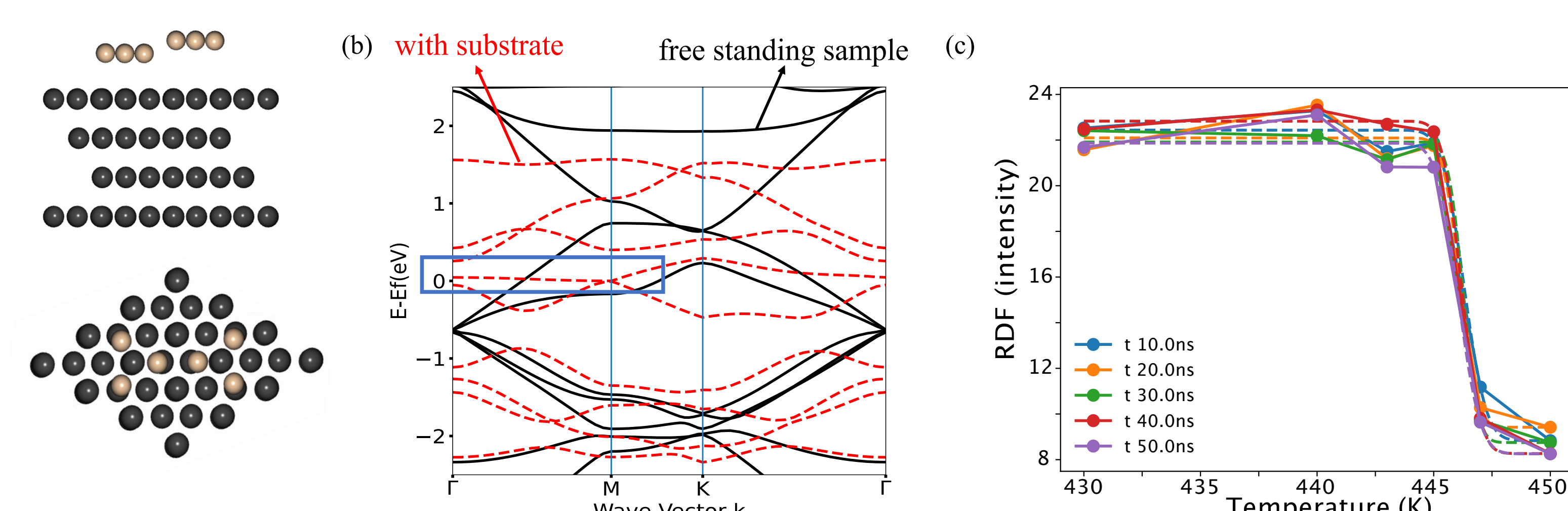


Figure 7. (a) Structural configuration and (c) RDF intensity as a function of temperature for buckled SiKL on a four-layer Ag(111) substrate. (b) Band structure of buckled SiKL grown on the Ag substrate (red dashed lines) compared with the free-standing sample (black solid lines).

## Band Diagram of Buckled SiKL

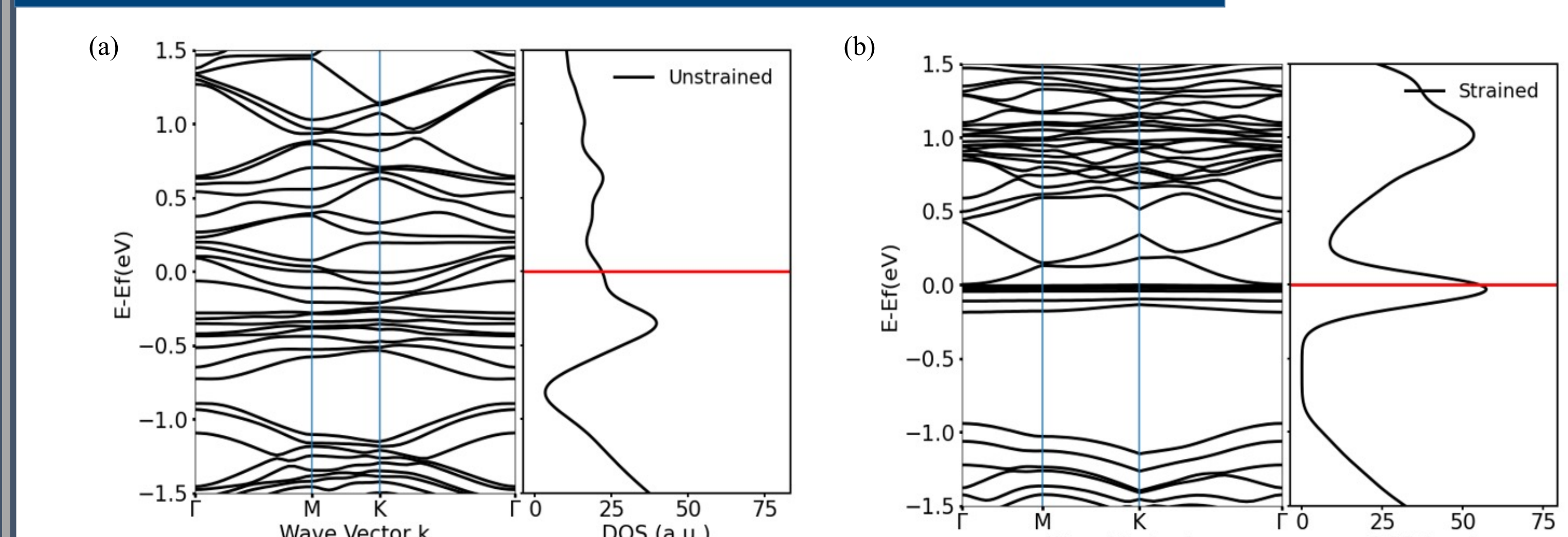


Figure 8. Band structures and density of states (DOS) of a  $6 \times 6 \times 1$  superlattice of buckled SiKL after AIMD simulations: (a) unstrained sample and (b) sample optimized under 0.1 biaxial strain.

## Acknowledgements

ASB and CW acknowledge financial support by the U.S. Department of Energy, Office of Science (grant DE-SC0023432) and computational resource support from UCLA's Institute for Digital Research and Education (IDRE), and the National Energy Research Scientific Computing Center (BES-ERCAP0033206, BES-ERCAP0025205, BES-ERCAP0025168, and BES-ERCAP0028072).